



# Green Synthesis of Aluminum Silicate and Aluminum Iron Oxide Nanocomposites for Industrial Applications

Muhammed Saad Shabir<sup>1</sup>, Hina Zain<sup>1\*</sup>, Moin Maqsood<sup>1</sup>, Aysha Bukhari<sup>2</sup>,  
and Ammara Nazir<sup>2</sup>

<sup>1</sup>Department of Chemistry, Superior University, Lahore, Pakistan

<sup>2</sup>Department of Chemistry, Minhaj University, Lahore, Pakistan

**Abstract:** Nano chemistry is revolutionizing the chemical industry. This research targets the green synthesis of Al-Si and Al-Fe nanocomposites and their application in the cement industry to produce durable cement coating. The nanocomposites were prepared by incorporating the green ingredients as reducing and stabilizing agents followed by the direct heating and calcination of the samples. The X-ray diffraction analysis and SEM were performed to confirm crystallinity and the nano-dimensional structure of the prepared nanocomposites. The SEM micrographs of Al-Si and Al-Fe nanocomposites provided the sizes as 15-37 nm and 17-61 nm, respectively. BET analysis revealed the surface area as 1.084 m<sup>2</sup>/g and 0.884 m<sup>2</sup>/g, respectively, for Al-Si and Al-Fe nanocomposites. These were applied in cement mortar and stability was checked for 07 and 28 days. The samples with 07 days of stability time showed an increase while the samples with 28 days showed a decrease in compressive strength.

**Keywords:** Nanocomposites, Cement Industry, Compressive Strength, Green Synthesis.

## 1. INTRODUCTION

Nanoscience has emerged as an outstanding field in the recent past and has been producing advancement in different departments of science, engineering, and technology. Nanomaterials have at least one dimension in the nanoscale, i.e., length or width, size, morphology, etc. There are several methods to prepare efficient and functional nano-surfaces that can help to reduce reaction times, do better yields, and produce durable materials. Sol-gel, chemical vapor deposition, hydrothermal procedures, green techniques, and Laser methods are some popular methods to produce nano-engineered substance [1]. Nanoparticles and nanocomposites are two important classes of nanomaterial that have been utilized in different industries to enhance the efficiency and capability of materials, i.e., cement, paints, coating, and many other industries. Nanoparticles like nano-silica, alumina, and titanium nanoparticles have improved the structure and function of numerous materials and surfaces. When two elements are combined, a composite is obtained which has more efficiency and

functionality than the individual particles. Recently, a widespread use of nanocomposites has been observed in the infrastructure department where they have contributed to producing comprehensive and functional surfaces with improved durability and versatile properties. The incorporation of silica and iron-based nanocomposites into cement has generated substantial interest due to their ability to enhance the mechanical, thermal, and durability characteristics of cementitious materials. Silica and iron-based nanocomposites have impacted very much on the properties of cement mortar like CO<sub>2</sub>-impregnated silica [2], titanium-coated silica [3], alumino-silicates, barium silicate [4], Fe/Al [5] and Fe/Cu [6] have enhanced the durability, compressive and mechanical strength. The modern surfaces containing nanocomposites have resolved the issues of cracks, fouling of surface, less durability, and unwanted photo-catalytic processes to some extent [7-9].

As demand is continues rising for sustainable, high-performance construction materials, exploring nanocomposites in cement manufacturing has

grown increasingly crucial. This research paper seeks to examine the importance of the inculcation of silica and iron-based nanocomposites in cement, emphasizing their capacity to boost the strength, durability, and environmental sustainability of concrete structures. Research is underway to improve the quality of the cement mortar and provide the best product for infrastructure strength [10, 11]. However, there is still a need for a more durable and functional surface, i.e., cement mortar which can enhance the lifetime of the material and avoid said issues to a maximum extent. Therefore, this topic has great potential for research and development of sustainable construction materials and practices.

## 2. MATERIALS AND METHODS

### 2.1. Preparation of *Azadirachta indica* Leaves Extract

Fresh and green leaves of *Azadirachta indica* were collected from the Lahore region and were washed with distilled water. 40 g of leaves were boiled in 350 ml distilled water for 30 minutes. The extract was cooled and filtered. The prepared extract was stored for further processing [12].

### 2.2. Preparation of Al-Si Nanocomposite

0.001 M  $\text{SiO}_2$  solution was added dropwise in 0.001 M  $\text{Al}(\text{OH})_3$  with constant stirring at room temperature. When the solution was homogenized the *Azadirachta indica* leaves extract was added in a ratio of 1:2 with constant stirring. A clear yellow solution was formed. It was kept in the oven for overnight at 90 °C, hard dry mass was obtained which was ground and calcination was done at 600 °C for 2 hours [13].

### 2.3. Preparation of Al-Fe Nanocomposite

0.001 M  $\text{FeCl}_3$  solution was mixed with 0.001 M  $\text{Al}(\text{OH})_3$  with constant stirring for 30 minutes at room temperature. When the solution was homogenized the *Azadirachta indica* leaves extract was added in a ratio of 1:2. The solution was turned black. It was then dried in an oven overnight at 100 °C. The dried mass was calcinated in an oven at 650 °C for three hours [12].

### 2.4. Characterization of Nanocomposites

Scanning electron microscopy (SEM) analysis was performed through Nova Nano SEM to evaluate the size and morphology of Al-Si and Al-Fe nanocomposites. X-ray diffractometer was also used to identify the synthesized nanocomposites. In addition to it, the EDX analysis was also performed to check the elemental composition of the nanocomposites.

Surface area analysis and adsorption capacity of nanocomposites were studied from BET analysis. It is the physical adsorption of gas molecules on a solid surface. The surface area can be calculated from the BET equation stated below.

$$1/W[(P_0/P) - 1] = 1/W_m C + C - 1/W_m C(P/P_0) \quad (1)$$

Samples were prepared for BET analysis. Nitrogen gas was used to check the adsorption level of the nanomaterial and to assess the possible sites available for adsorption purposes. The temperature was kept at 77 K which is the standard temperature for performing the analysis. Powdered samples were used for the analysis. The experiment was performed at the COMSATS University Islamabad, Lahore Campus.

### 2.5. Compressive Strength of Cement Mortar

To study the effect of nanocomposites on the compressive strength of cement mortar was studied. Four samples of cement mortar cubes were prepared by mixing sand and cement in a 2:1 ratio. Each nanocomposite in the concentration of 0.1% and 0.15% of the total weight of mortar was added. Samples were mixed thoroughly in water and poured into the 4 cm × 4 cm wooden molds for setting prepared. A control sample was also prepared without adding nanocomposites. Compressive strength testing was done on cubes after 7 and 28 days of setting [7, 8]. The instrument used for the testing of the cubes was Compression Testing Machine from Islamia University of Bahawalpur. The cubes were kept in the machine one by one and a pressure was released by the presser within the machine. The reading on the digital meter was the compressive strength of the cube which it was bearing inside the machine.

### 3. RESULTS AND DISCUSSION

#### 3.1. SEM and EDX of Al-Si and Al-Fe Nanocomposites

The SEM images obtained revealed the size of the nanoparticles. Figure 1(a) shows that the silica nanoparticles were 15-37 nm in size with the morphology of rod shape embedded in the aluminum matrix [14]. The shape looks more like a core-shell nanoparticle in which silica nanoparticles behave like the core and aluminum matrix as a shell. The per unit percentage of silica nanoparticles was high in the aluminum matrix. SEM micrograph shows a strong interfacial interaction between the aluminum and silicon nanocomposites. There also exists a pore formation and it has a direct relation with the size of silica nanoparticles. In Figure 1(b), iron nanoparticles can be seen evenly distributed at different interfacial angles with the aluminum nanoparticles. The morphology of the iron nanoparticles can be seen as cubic and spherical

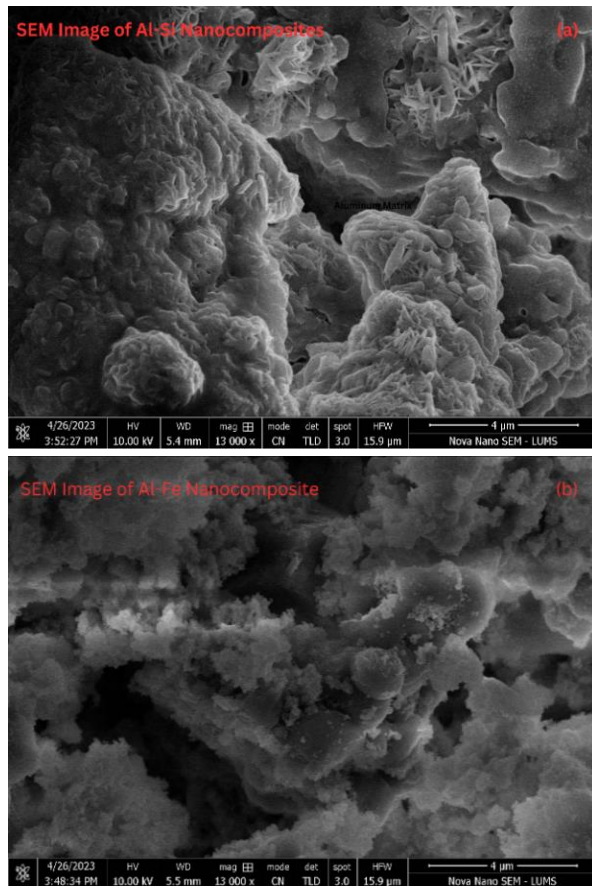


**Fig. 1.** (a) SEM image of Al-Si Nanocomposite, (b) SEM image of Al-Fe Nanocomposite.

**Table 1.** Energy-Dispersive X-Ray Spectroscopy results of Al-Si Nanocomposites.

Sr. No.	Element	Percentage (%)
1	Carbon (C)	22.08
2	Oxygen (O)	41.33
3	Magnesium (Mg)	2.62
4	Aluminum (Al)	0.11
5	Silicon	2.92

**Table 2.** Energy-Dispersive X-Ray Spectroscopy results of Al-Fe Nanocomposites.

Sr. No.	Element	Percentage (%)
1	Carbon (C)	23.24
2	Oxygen (O)	28.32
3	Magnesium (Mg)	4.62
4	Aluminum (Al)	0.12
5	Silicon (Si)	1.36
6	Iron (Fe)	4.29
7	Calcium (Ca)	9.51
8	Potassium (K)	15.4

particles in contact with the aluminum surface and dispersed in a good manner. The bonding between the aluminum and iron nanoparticles as well as dispersion can be seen across the micrograph. Particle sizes ranging from 17-61 nm are present [15]. The pore density is very low in between the iron and aluminum nanoparticles. This in turn happens good for the mechanical and functional properties of the material.

The elemental breakup of the nanocomposites obtained from the SEM-EDX analysis is presented in Table 1 for Al-Si nanocomposites and in Table 2 for Al-Fe nanocomposites.

#### 3.2. XRD Analysis of Al-Si and Al-Fe Nanocomposites

X-ray diffraction spectrum of Al-Si nanocomposites is shown in Figure 2(a), the peaks observed at  $28.3^\circ$ ,  $34.1^\circ$ ,  $40.6^\circ$ ,  $50.2^\circ$ , and  $66.4^\circ$  correspond to the plane of quartz (001), kaolinite (001), muscovite (001), kaolinite (110) and (102), respectively, and agree with the JCPDS file (46-1045), (29-1488), (39-1484) and (29-1488) for both the phases of kaolinite. These planes or diffraction angles correspond to different mineral compositions of the Alumino-

silicate nanocomposites. These results show the presence of different crystallographic planes of aluminum oxide and iron oxide nanoparticles. The major phases include kaolinite, feldspar, andalusite, and quartz. These different phases exist due to the difference in the ratio of  $\text{Al}_2\text{O}_3$  and  $\text{SiO}_2$ . While in Figure 2(b), the XRD peaks observed at  $28.36^\circ$  (001 planes of Boehmite, JCPDS file number, 21-1307); the peaks at  $40.56^\circ$ ,  $50.44^\circ$ ,  $66.8^\circ$  and  $73.96^\circ$  correspond to hematite (024, 001, 014 planes) and maghemite (001, 110, 113) with JCPDS file numbers as 33-0664 and 39-1346, respectively.

### 3.3 BET Analysis of Al-Si and Al-Fe Nanocomposites

Two Different types of adsorption isotherms were obtained showing adsorption of the materials against the relative pressure (Figure 3). As the amount of the material is enhanced, the adsorption also becomes greater.

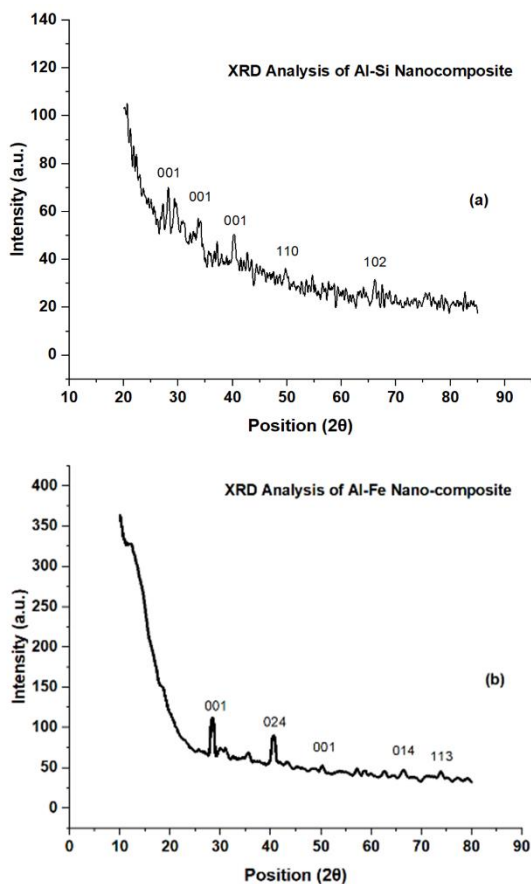


Fig. 2. (a) XRD Pattern of Al-Si nanocomposite, (b) XRD Pattern of Al-Fe nanocomposite.

### 3.3.1. Adsorption analysis of Al-Si and Al-Fe nanocomposites through BET

In order to calculate the surface area of the nanocomposites Equation (1) is employed. To find the surface area, a graph is plotted between  $1/[W((P_0/P) - 1)]$  on the y-axis and relative pressure  $p/p_0$  on the x-axis. Surface area can also be found through putting the available information. The total surface area of the Al-Si and Al-Fe nanocomposites was calculated as  $1.084 \text{ m}^2/\text{g}$  and  $0.884 \text{ m}^2/\text{g}$ , respectively. Another important factor is the total pore volume which is less than 2.6 nm of size in both cases and recorded as  $4.528 \times 10^{-4}$  and  $3.37 \times 10^{-4}$ . The micropore area and volume were recorded as 0.00 cc/g. The surface area calculated through multi-point BET is  $1.084 \text{ m}^2/\text{g}$  and  $0.884 \text{ m}^2/\text{g}$ , for Al-Si and Al-Fe nanocomposite, respectively [16, 17].

In Figure 4(a), the isotherm represents the type II isotherm as given by IUPAC. There are a total of 06 types of isotherms which denote different

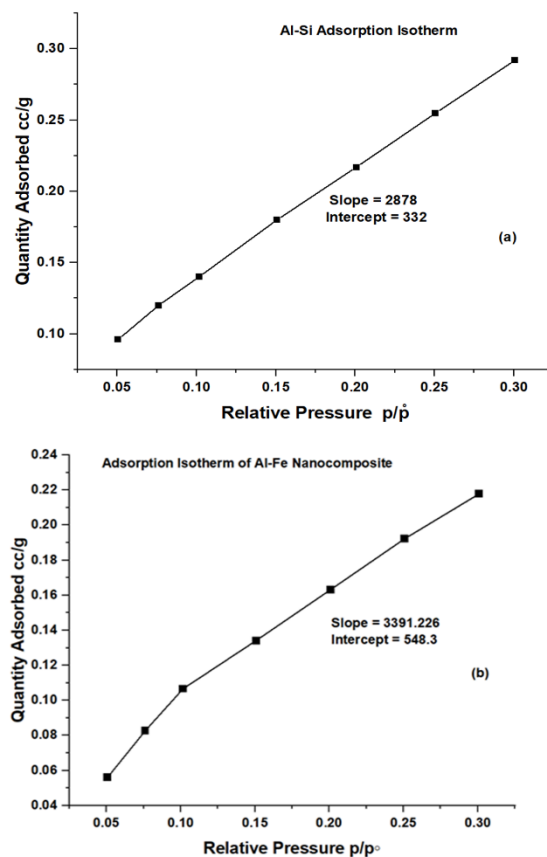


Fig. 3. (a) Adsorption Capacity of Nanocomposites Al-Si, (b) Adsorption Capacity of Al-Fe Nano-composite.

characteristics of adsorption of different materials [18]. The type II isotherm successfully explains the adsorption on porous monolayer materials at low pressure and on mesoporous multilayer materials at high pressure with no hysteresis. The process is termed Multiple Site Adsorption in which adsorbing sites are the unit sites of total adsorbing area. In Figure 4(b), the isotherm is more likely the type III isotherm which explains the more adsorbate-adsorbate reaction than the adsorbent and adsorbate reaction.

### 3.3.2. Compressive strength analysis of nanocomposite added cement mortar samples

After 07 days and 28 days of setting time, the cement mortar samples were tested. The mortar sample with both nanocomposites after 07 days of setting time showed high compressive strength as compared to the 28-day setting time.

The results mentioned in Table 3 show the

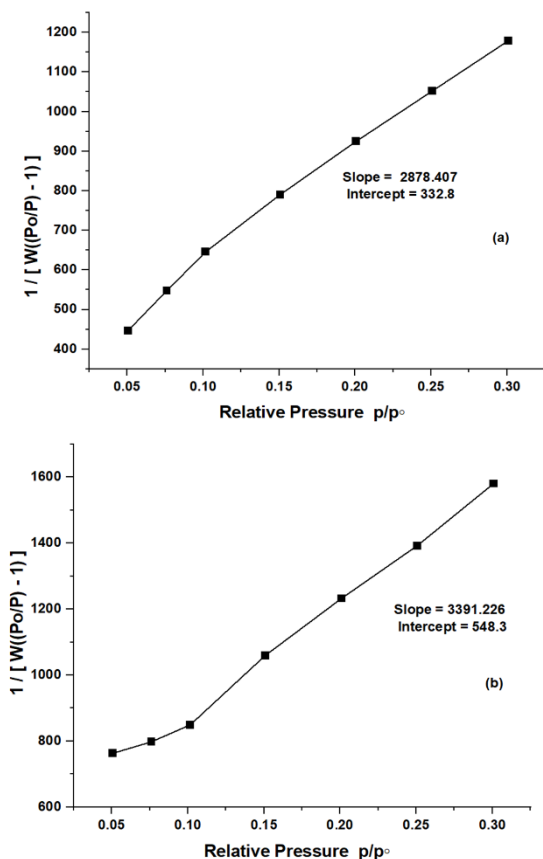


Fig. 4. (a) Plot of Al-Si Nano-Composites to determine surface area, (b) Plot of Al-Fe Nanocomposites to determine surface area.

compressive strength after 07 days of stability time, it is suggested that ratios for both the nanocomposites helped in accelerating the binding capacity of mortar. of the cement mortar as compared to the control sample. The application of alumino-silicate and aluminum iron oxide nanocomposite was done in the cement mortar to check the change in the compressive strength of the cement mortar. Alumino-silicate and aluminum iron oxide incorporated cement mortar showed an increase in the compressive strength of the cement mortar in comparison with the control group with no addition of nanocomposites. It can also be inferred that increasing the percentage of the nanocomposites caused the increase in strength. Control sample showed strength of 26.3 MPa while that of both nanocomposites showed more strength at 0.1% and 0.15%. This is due to an increase in the formation of calcium silicate hydrate gel through which the voids and spaces are filled, and the structure densifies [19, 20].

Table 4 shows that after the curing time of 28 days, there was a decrease in the compressive strength which occurred due to weak bonding attraction developed between the particles of the cement and nanocomposite. It has been observed

Table 3. Compressive strength increases after 07 days of stability time.

Sr. No	Nanocomposite	Percentage of nano-composite Added	07 Days Strength Comparison (MPa)	Load (KN)
1	Control	0%	26.3	263
2	Al-Si	0.1%	35.2	352
3	Al-Si	0.15%	36.3	363
4	Al-Fe	0.1%	33.4	334
5	Al-Fe	0.15%	41.3	413

Table 4. Compressive strength increases after 28 days of stability time.

Sr. No	Nanocomposite	Percentage of nano-composite Added	28 Days Strength Comparison (MPa)	Load (KN)
1	Control	0%	28.7	287
2	Al-Si	0.1%	16.43	164.3
3	Al-Si	0.15%	21.22	212.2
4	Al-Fe	0.1%	21.48	214.8
5	Al-Fe	0.15%	14.65	146.5

in the previously published research, that 07 days cured cement mortar samples had more compressive strength than the 28 days cured cement [21, 22]. The composition of both the nanocomposites with 0.1% and 0.15% showed a decrease in the strength and on both cases the strength with all composition of Al-Si and Al-Fe was less than the strength of control. At early stages, the pozzolanic reaction caused the formation of calcium-silicate-nanocomposite - cement gel causing denser structure. Later continuous hydration may have caused the breakage of the gel structure causing more cracks in the cement mortar thereby causing reduction in the denser structure.

#### 4. CONCLUSIONS

This research paper aimed at the preparation of Aluminum Silicate and Aluminum Iron Oxide nanocomposite through the green route followed by SEM, EDX, XRD, and BET characterization with their industrial application in the cement industry. The results obtained through characterization confirmed the nano dimensions of the materials. Furthermore, the prepared nanocomposites were applied in the cement mortar, and after 07 and 28 days of stability time, the compressive strength increase was observed in the samples cured for 07 days. Reduction in 28 days of cured samples' compressive strength was observed due to weak bonding attraction between the nanocomposites and cement mortar. The more strength at 07 days may be due to the filling up of the spaces and interaction sites of the cement mortar by the nanocomposites and later on agglomeration or leeching out of the nanocomposite caused lowering of strength.

#### 5. ACKNOWLEDGEMENTS

GC University Lahore and Minhaj University Lahore provided instruments, chemicals and labs for research purposes.

#### 6. CONFLICT OF INTEREST

The authors declare no conflict of interest.

#### 7. REFERENCES

1. N. Baig, I. Kammakam, and W. Falath. Nanomaterials: A review of synthesis methods, properties, recent progress, and challenges. *Materials Advances* 2(6): 1821-71 (2021).
2. T.M. Jassam, K. Kien-Woh, B. Lau, and M. Yaseer. Novel cement curing technique by using controlled release of carbon dioxide coupled with nanosilica. *Construction and Building Materials* 223: 692-704 (2019).
3. P. Sikora, K. Cendrowski, A. Markowska-Szczupak, E. Horszczaruk, and E. Mijowska. The effects of silica/titania nanocomposite on the mechanical and bactericidal properties of cement mortars. *Construction and Building Materials* 150: 738-46 (2017).
4. H.A. Abdel-Gawwad, K.A. Metwally, and T.A. Tawfik. Role of barium carbonate and barium silicate nanoparticles in the performance of cement mortar. *Journal of Building Engineering* 44: 102721 (2021).
5. F. Gulshan, and K. Okada. Preparation of alumina-iron oxide compounds by coprecipitation and gel evaporation methods and their characterization. *Journal of Engineering Research* 3: 1-8 (2015).
6. S.R. Dhruval, N. Pai, S.S. Dhanwant, B. Hussein, S. Nayak, C.V. Rao, A. Kumar, and M. Janakaraj. Rapid synthesis of antimicrobial Fe/Cu alloy nanoparticles using Waste Silkworm Cocoon extract for cement mortar applications. *Advances in Natural Sciences: Nanoscience and Nanotechnology* 11(2): 025006 (2020).
7. S. Kawashima, P. Hou, D.J. Corr, and S.P. Shah. Modification of cement-based materials with nanoparticles. *Cement and Concrete Composites* 36: 8-15 (2013).
8. A.S. Kadhim, A.A. Atiyah, and S.A. Salih. Properties of self-compacting mortar containing nano cement kiln dust. *Materials Today: Proceedings* 20: 499-504 (2020).
9. K.H. Younis, and S.M. Mustafa. Feasibility of using nanoparticles of SiO<sub>2</sub> to improve the performance of recycled aggregate concrete. *Advances in Materials Science and Engineering* 2018: 1512830 (2018).
10. N.H.A.S. Lim, H.M. Hosseini, M.M. Tahir, M. Samadi, and A.R.M. Sam. Microstructure and strength properties of mortar containing waste ceramic nanoparticles. *Arabian Journal for Science and Engineering* 43: 5305-13 (2018).
11. M. Kumar, M. Bansal, and R. Garg. An overview of beneficiary aspects of zinc oxide nanoparticles on performance of cement composites. *Materials Today: Proceedings* 43: 892-898 (2021).
12. M. Pattanayak, and P. Nayak. Green synthesis and

- characterization of zero valent iron nanoparticles from the leaf extract of *Azadirachta indica* (Neem). *World Journal of Nano Science and Technology* 2(1): 6-9 (2013).
13. Y. Li, X. Zhang, C. Shang, X. Wei, L. Wu, X. Wang, W.D. Wu, X.D. Chen, C. Selomulya, D. Zhao, and Z. Wu. Scalable synthesis of uniform mesoporous aluminosilicate microspheres with controllable size and morphology and high hydrothermal stability for efficient acid catalysis. *ACS Applied Materials and Interfaces* 12(19): 21922-35 (2020).
  14. V.T. Cong, K. Gaus, R.D. Tilley, and J.J. Gooding. Rod-shaped mesoporous silica nanoparticles for nanomedicine: recent progress and perspectives. *Expert Opinion on Drug Delivery* 15(9): 881-92 (2018).
  15. A. Mahapatra, B. Mishra, and G. Hota. Adsorptive removal of Congo red dye from wastewater by mixed iron oxide–alumina nanocomposites. *Ceramics International* 39(5): 5443-51 (2013).
  16. A. Chatterjee, J.K. Basu, and A.K. Jana. Alumina-silica nano-sorbent from plant fly ash and scrap aluminium foil in removing nickel through adsorption. *Powder Technology* 354: 792-803 (2019).
  17. F. Gulshan, and K. Okada. Preparation of alumina-iron oxide compounds by coprecipitation and gel evaporation methods and their characterization. *Journal of Engineering Research* 3: 1-8 (2015).
  18. M.A. Al-Ghouti, and D.A. Da'ana. Guidelines for the use and interpretation of adsorption isotherm models: A review. *Journal of Hazardous Materials* 393: 122383 (2020).
  19. D.E. Ramírez-Arreola, C.S. Rosa, N.B. Haro-Mares, J. A. Ramírez-Morán, A.A. Pérez-Fonseca, and J.R. Robledo-Ortiz. Compressive strength study of cement mortars lightened with foamed HDPE nanocomposites. *Materials and Design* 74: 119-24 (2015).
  20. W.N. Al-Rifaie, and W.K. Ahmed. Effect of nanomaterials in cement mortar characteristics. *Journal of Engineering Science and Technology* 11(9): 1321-32 (2016).
  21. S.A. Zareei, F. Ameri, F. Dorostkar, and M. Ahmadi. Rice husk ash as a partial replacement of cement in high strength concrete containing micro silica: Evaluating durability and mechanical properties. *Case Studies in Construction Materials* 7: 73-81 (2017).
  22. Y. Fang, Y. Sun, M. Lu, F. Xing, and W. Li. Mechanical and Pressure-sensitive Properties of Cement Mortar Containing Nano-Fe<sub>2</sub>O<sub>3</sub>. *Proceedings of the 4<sup>th</sup> Annual International Conference on Material Engineering and Application (ICMEA 2017)*: 206-210 (2018).

